ARTICLE IN PRESS

Physica A xxx (xxxx) xxx

Contents lists available at ScienceDirect

Physica A

journal homepage: www.elsevier.com/locate/physa

Ordering dynamics in the voter model with aging

Antonio F. Peralta, Nagi Khalil, Raúl Toral *

IFISC (CSIC-UIB), Instituto de Física Interdisciplinar y Sistemas Complejos, Campus Universitat de les Illes Balears, E-07122 Palma de Mallorca, Spain

ARTICLE INFO

Article history:
Available online xxxx

Keywords:
Voter model
Aging
Non-Markovian dynamics

ABSTRACT

We study theoretically and numerically the voter model with memory-dependent dynamics at the mean-field level. The "internal age", related to the time an individual spends holding the same state, is added to the set of binary states of the population, such that the activation probability p_i for attempting a change of state has an explicit dependence on the internal age i. We derive a closed set of integro-differential equations describing the time evolution of the fraction of individuals with a given state and internal age, and from it we obtain analytical results characterizing the behavior of the system close to the absorbing states. In general, different internal age-dependent activation probabilities p_i have different effects on the dynamics. In the case of "aging", i.e. p_i being a decreasing function of its argument i, either the system reaches consensus or it gets trapped in a frozen state, depending on whether the limiting value p_∞ is zero or positive, and on the rate at which p_i approaches p_∞. Moreover, when the system reaches consensus, the fraction $x(t)$ of nodes not holding the consensus state may decay exponentially with time or as a power-law, depending again on the specific details of the functional form of p_i. For the case of "anti-aging", when the activation probability p_i is an increasing function of i, the system always reaches a steady state with coexistence of opinions. Exact conditions for having one or another behavior, together with the equations and explicit expressions for the power-law exponents, are provided.

1. Introduction

Agent-based binary-state models are commonly used to study the effect that simple individual dynamical rules may have on the collective behavior of a system. Typical examples include modeling the spreading of diseases [1,2], the time evolution of the number of speakers of a given language [3–6], the evolution of prices in financial markets [7–14], or the dynamics of opinion formation in a population of individuals [15–17]. As a prominent case of the latter, the voter model [18–20] and variants thereof [21], by which an agent adopts with some probability the state of a randomly chosen neighbor, are widely used when the mechanism at hand is that of imitation. Beyond its potential applications, the voter model has become a paradigm in the field of non-equilibrium statistical physics. It is defined by very simple rules, and explicit solutions can be given in some particular cases, yet it is capable of showing very rich behavior, including phase transitions, characterized by critical exponents, power-law correlations, finite-size scaling, tricritical behavior, etc. [22,23]. Recent studies of the voter model include the effect of a network structure [24,25], non-linear or group interactions [26–30], coevolution dynamics [31–35], more than two states [36,37], the effect of zealots [38] and contrarians [39], etc.

* Corresponding author.
E-mail addresses: afperalta@ifisc.uib-csic.es (A.F. Peralta), raul@ifisc.uib-csic.es (R. Toral).

https://doi.org/10.1016/j.physa.2019.122475
0378-4371/

Please cite this article as: A.F. Peralta, N. Khalil and R. Toral, Ordering dynamics in the voter model with aging, Physica A (2019) 122475, https://doi.org/10.1016/j.physa.2019.122475.

A fundamental aspect of the agent-based binary-state models is the memory the constituents of the system have [40], and how this affects the dynamical rules that define the model. A clear example is the framework of non-Poissonian infection processes in epidemic spreading [41–43], where the infection of an individual depends on the times each one of its neighbors became infected [44]. This is because the rate at which one transmits a disease is not independent of the time one has been infected. In most cases of binary-state models a Markovian assumption is postulated which implies that the probability of changing state is independent of the past history of events of the individuals, that is to say neglecting memory effects by including Poissonian processes. This is of course a simplification that can be justified in many phenomena and it makes the mathematical treatment a lot easier [45,46], but it may be less realistic in other cases. In this context, one of the objectives of the present work is to provide a consistent mathematical description of the voter model including memory effects, namely by making the probability of changing opinion of agents dependent on their "persistence time", defined as the time elapsed since the last change of state [47,48].

One of the main questions addressed by the voter model is whether the imitation rule leads to a situation of consensus, with all agents (or at least, a significant majority) adopting the same value of the binary state [49–51]. The answer to this question is sometimes counter-intuitive. Although it would appear, for example, that an increase in the connections amongst the agents should favor consensus, a detailed analysis shows that for an effective dimensionality of the connectivity network greater than two, the system is not able to sustain a consensus state in the thermodynamic limit. The problem has been also addressed when including memory effects. Stark et al. [47] introduced increasing inertia, otherwise known as "aging" [52], as a mechanism that reduces the probability of an agent to copy the state of another one. Aging can then be related to an increase of the inflexibility in the copying mechanism [53]. Again, it would seem naively that reducing the number of interactions amongst agents should impede the reaching of consensus, but it was shown that exactly the opposite happens, namely the consensus is reached more easily in such a scenario of aging. In a recent paper by some of us [54,55], it was shown that the inclusion of aging in the noisy version of the voter model [7,56,57] induces a state of imperfect consensus that remains in the thermodynamic limit. Another related study of the noiseless voter model [48] focused on the distribution $C(t)$ of the time t between individual changes of states, which in turn is related with a probability of interaction p_i that depends on the persistence time i of the individual. The conclusion of [48], sustained from the analysis of extensive numerical simulations, was that a particular functional form of $p_i \sim b/i$ induces a power-law dependence $C(t) \sim t^{-\beta}$, which has been observed in real datasets, for example in human communications [58,59]. This power-law is similar to the ones observed in the approach to consensus in low-dimensional lattices, but it shows a strong dependence on the details of the activation probability. The main objective of this paper is to analyze this problem and to derive the relations in [47,48], among others, from an analytical point of view. We also aim to give a well constructed theoretical framework for aging, which has been studied together with network structure in several recent works [52,60,61] but mainly computationally, due to the difficulties encountered in the mathematical description.

The outline of the paper is as follows. In Section 2 we introduce the voter model including memory effects. We consider two specific forms of the activation probability, rational and exponential functions of the persistence time, which depend on several parameters, so as to cover the phenomenology observed in the literature. Section 3 includes a summary of the main results present in the literature about the dynamical behavior of the system close to the absorbing states. In Section 4 the dynamical equations of the mean fraction of agents with a given state and persistence time are obtained under a mean field description and its steady-state analyzed. Section 5 contains the main results of the work. First, a closed set of integro-differential equations describing the system close to the absorbing states is derived. Second, an approximate analysis of the previous description is carried out, providing explanation to the numerical findings. Some more technical details of the calculations are given in Appendices A and B. Finally, Section 6 includes a summary of the main results.

2. Model

The voter model implements in arguably the simplest way the herding mechanism for the evolution of binary-state systems. In the original version one considers a system formed by N individuals or agents. Agents are located in the nodes of a network and are connected by undirected, bidirectional, links. Two connected individuals are said to be "neighbors". The network is single connected, meaning that every node can be reached from any other node by a sequence of links. Each individual $k = 1, \ldots, N$ holds a binary-state (spin) variable $s_k = \pm 1$. Several interpretations can be given to this binary variable, but its exact meaning does not concern us in this paper. For example, the voter model or variants of it have been used to represent the optimistic/pessimistic state of a stock market broker [7], the language A/B used by a speaker [3,6], or the direction of the velocity right/left in a one-dimensional model of active particles [62], etc. Those variables evolve over time by the following (stochastic) rules:

(i) An individual k is selected at random amongst the N possibilities.
(ii) The selected individual copies the state $s_k = s_{k'}$ of another individual k' chosen also at random between the set of neighbors of k.

In this random updating scheme, every time an individual is chosen for updating, time t increases by one unit, while N updates constitute one Monte Carlo step (MCS).

In the aging version of the voter model the above rules are modified such that the herding mechanism occurs only with an *activation probability* p_{i_k} that depends on the *internal age* i_k of the selected individual. The internal age $i_k = 0, 1, 2, \ldots$

Please cite this article as: A.F. Peralta, N. Khalil and R. Toral, Ordering dynamics in the voter model with aging, Physica A (2019) 122475, https://doi.org/10.1016/j.physa.2019.122475.

of individual k stands for the number of updates elapsed since its last change of state, or the number of failed updates. As the individuals have the same probability of being chosen for an update, the internal age of an individual will be, on average, equal to its persistence time, or time since the last change of state. The inclusion of the internal age (henceforth, simply *age*) instead of the persistence time simplifies the mathematical treatment and will be considered throughout the paper.

More explicitly, the model is reproduced in the simulations by modifying the last step as follows:

(ii) The selected individual copies **with probability $\mathbf{p_{i_k}}$** the state $s_k = s_{k'}$ of another individual k' chosen at random between the set of neighbors of k. If the selected individual changes state $s_k \to -s_k$, then its internal age resets to zero $i_k \to 0$; otherwise it increases in one unit $i_k \to i_k + 1$. Initially, all internal ages are set to zero.

The standard (no aging) voter model is recovered taking $p_i = 1$. Here, for the sake of concreteness and mathematical treatment, we have considered the following two functional forms for the activation probability:

1. The first functional form is a rational function of the age,

$$p_i = \frac{p_\infty i + p_0 c}{i + c}, \quad i = 0, 1, 2, \ldots \tag{1}$$

where p_0, $p_\infty \in [0, 1]$ and $c > 0$ are constants. If $p_0 > p_\infty$, the probability of interaction decreases with age, a typical aging situation. The opposite occurs if $p_0 < p_\infty$, as the activation probability increases with age. This can be interpreted as "anti-aging" or "rejuvenating" where as nodes remain longer in the same state they become more prone to change state. This aging form, with $p_\infty = 0$, is basically the form considered in [48] and that has been shown to induce features observed in several real-world systems, such as power-law inter-event time distributions. If $p_0 = 1$ and $p_\infty > 0$, this reproduces qualitatively the form used in Ref. [47]. In that paper, the activation probability p_i, equivalent to $1 - \nu_i$ with ν_i being the "inertia", decreases linearly from $p_0 = 1$ up to a final constant, non-null value p_∞, but at a finite value of i.
2. The second form we adopt is an exponential function of the age,

$$p_i = (p_0 - p_\infty)\lambda^i + p_\infty, \quad i = 0, 1, 2, \ldots \tag{2}$$

with the same meaning as before for p_0 and p_∞, and $\lambda \in [0, 1]$ is a parameter. Besides providing a functional form that varies much more rapidly with age than the rational function given by Eq. (1) (and we will see that our analysis predicts that the speed of approaching the asymptotic value p_∞ determines the final collective state), this exponential form has been chosen for mathematical simplicity as it will allow us to perform analytical calculations.

3. Dynamical behavior. Absorbing states

When one individual changes its state after copying the state of one of its neighbors, the overall result can be that the total number of neighbors with which it shares the same state either increases, decreases or remains the same. A question of interest is whether by iteration of the dynamical rules a "consensus", or fully ordered, state in which all agents share the same state, either $+1$ or -1, is finally achieved. One can argue that the stochastic rules permit eventually to reach any possible configuration of states. Therefore, when any of the particular consensus states $s_k = +1, \forall k$ or $s_k = -1, \forall k$ is reached, there cannot be further evolution and the dynamics stops. Those fully ordered states are "absorbing" states, as once the system has reached one of them, the number of individuals holding a particular state does not vary with time. It seems, therefore, that the ultimate fate of the system is to reach consensus in one of the two absorbing states, with all nodes sharing the same value. Whether the $+$ or the $-$ state is reached depends exclusively on the initial conditions and the particular realization of the stochastic dynamics. While this is certainly true for any system with a finite number N of agents, it is enlightening to analyze the way the consensus state is reached and the dependence with system size of the average time to reach that state. Two different measures have been introduced to study the approach to order: the magnetization $m(t) = N^{-1}\sum_{k=1}^{N} s_k(t)$ that takes values $m = \pm 1$ in the ordered states, and the density $\rho(t)$ of active links, defined as the fraction of links that join nodes in different states. In the ordered states, the magnetization can be $m = +1$ or $m = -1$, while $\rho = 0$ in both absorbing states. The existence of absorbing states then ensures that $\lim_{t\to\infty} m(t) = \pm 1$ and $\lim_{t\to\infty} \rho(t) = 0$ for any finite system.

There is a significant difference between the aging and non-aging versions of the model. In the non-aging version the approach to the absorbing state depends crucially on the spatial dimension d. If $d > 2$ it is observed that the density of active links[1] has a fast transient to a plateau value ρ^* (for $d \to \infty$, i.e. all-to-all connectivity, $\rho^* = \rho(0)$) and it fluctuates around it until a large fluctuation brings the system to the absorbing state $\rho = 0$ at a time T. This time is a stochastic variable whose mean value scales as $\langle T\rangle \sim N$ for $d > 2$, see also [63], where the probability distribution of T is obtained for $d \to \infty$. Therefore, larger systems stay longer in an *active* state until a large fluctuation brings them to the absorbing state. As we take the thermodynamic limit $N \to \infty$, it results that $T \to \infty$ and the system does not order at all in a finite time. If we average over initial conditions and realizations of the dynamics, we find an exponential decay $\langle\rho(t)\rangle = \rho^* e^{-t/\tau}$,

[1] A similar qualitative behavior is observed for the magnetization. In fact, for the all-to-all connectivity considered later in this paper, one has the relation $\rho(t) = \frac{1}{2}\left[1 - m(t)^2\right]$, although in other networks $\rho(t)$ must be considered as an independent variable.

Please cite this article as: A.F. Peralta, N. Khalil and R. Toral, Ordering dynamics in the voter model with aging, Physica A (2019) 122475, https://doi.org/10.1016/j.physa.2019.122475.

with $\tau \propto \langle T \rangle$. As mentioned, in the thermodynamic limit when $\langle T \rangle = \infty$, we obtain $\langle \rho(t) \rangle = \rho^*$, or absence of order. If we take first the limit $t \to \infty$ and then the limit $N \to \infty$ we obtain otherwise $\lim_{N\to\infty} \lim_{t\to\infty} \langle \rho(t) \rangle = 0$. If the spatial dimension is $d \leq 2$ the decay to the absorbing state occurs very differently. One does not observe that $\rho(t)$ fluctuates around a plateau value, but rather $\rho(t)$ decreases on average for any realization even for large system sizes. As a consequence, in the thermodynamic limit, it is predicted that $\lim_{t\to\infty} \lim_{N\to\infty} \langle \rho(t) \rangle = 0$. The exact time dependence depends on the dimension as $\lim_{N\to\infty} \langle \rho(t) \rangle = (\log t)^{-1}$ for $d = 2$ and $\lim_{N\to\infty} \langle \rho(t) \rangle = t^{-1/2}$ for $d = 1$ [49–51].

The phenomenology in the aging version was described in [48] for particular forms of the activation probability. It was observed that if p_i follows a similar dependence as given by Eq. (1) with $p_\infty = 0$, then the approach to the absorbing states is described by a power-law $\lim_{N\to\infty} \langle \rho(t) \rangle = t^{-\beta}$, for large spatial dimensions. Furthermore, in a fully-connected network it was observed numerically that the exponent β of the power-law decay agreed within the numerical accuracy with the parameter $b \equiv p_0 c$ of Eq. (1).[2] This indicates that in the presence of this type of aging, the system always orders, contrarily to the non-aging version. In this paper we offer an explanation of this behavior.

4. The dynamical equations

We now derive the mean-field dynamical equations of the stochastic process defined in Section 2. In the derivation we restrict ourselves to the all-to-all (or fully connected) network in which all nodes are neighbors. The mathematical description in the case of a more complex network structure in the interactions between nodes is a further complication [24] and it is left for future studies [60,61]. In the all-to-all setup, all the information needed to implement the stochastic update rules is contained in the set $S \equiv \{n_i^\pm\}_{i=0}^\infty$ of the numbers of individuals with internal age i holding states ± 1 [47]. The global variables for the total number of up and down spins are $n = \sum_{i=0}^\infty n_i^+$ and $N - n = \sum_{i=0}^\infty n_i^-$. Note, however, that not all variables of the state S are independent, since they must satisfy the constraint $\sum_{i=0}^\infty (n_i^+ + n_i^-) = N$. Hence, it is useful to consider an alternative representation of the system in terms of independent variables, for instance by using the variable n and obviating $n_0^\pm$, as $S_n \equiv \left(n, \{n_i^+\}_{i=1}^\infty, \{n_i^-\}_{i=1}^\infty\right) = \left(n, n_1^+, n_2^+, \ldots, n_1^-, n_2^-, \ldots\right)$. In this representation $n_0^\pm$ are given by $n_0^+ = n - \sum_{i=1}^\infty n_i^+$ and $n_0^- = N - n - \sum_{i=1}^\infty n_i^-$.

In order to derive the dynamical equations of the global state of the system S_n, we must include with their respective probabilities all events that induce changes in S_n. Every time an individual changes its state or age, there is a change in the set of variables S_n. The change can occur in different ways and with different probabilities. We now spell in detail the possibilities and their effects on the variables.

(1) Consider that at time t the chosen individual k is in state $s_k = +1$ and has age $i_k = i$ and that as a result of the interaction it switches to $s_k = -1$ and, hence, its age is reset to $i_k = 0$. The probability of this event is equal to the probability, $\frac{n_i^+}{N}$, of choosing an individual with age i and state $+$, multiplied by the age-dependent probability, p_i, that activates the copying (herding) mechanism, and multiplied by the probability $\frac{N-n}{N}$ that the randomly selected neighbor is in the opposite state. Altogether, the probability is $\frac{n_i^+}{N} p_i \frac{N-n}{N} \equiv \frac{1}{N}\Omega_{1,i}$. When the switching of state occurs, if $i > 0$ we have $n_i^+ \to n_i^+ - 1$ and $n \to n - 1$, while if $i = 0$ the only change is $n \to n - 1$ (remember that $n_0^\pm$ are not a part of the set S_n).

(2) This is similar to the previous case but now the chosen individual is initially in state $s_k = -1$. The probability of switching is $\frac{n_i^-}{N} p_i \frac{n}{N} \equiv \frac{1}{N}\Omega_{2,i}$. When the switching of state occurs, if $i > 0$ we have $n_i^- \to n_i^- - 1$ and $n \to n + 1$, while if $i = 0$ the only change is $n \to n + 1$.

(3) Consider that at time t the chosen individual k has $s_k = +1$ and age $i_k = i$, but that now it keeps its current state $s_k = +1$. This event happens with a probability equal to the probability of choosing an individual in state $+1$ with age i, $\frac{n_i^+}{N}$, multiplied by the probability that it does not switch, which can arise either because the copying mechanism was not activated, with probability $1 - p_i$, or it was activated, probability p_i, but the selected neighbor was also in the state $+1$, with probability $\frac{n}{N}$. Altogether, the probability is $\frac{n_i^+}{N}\left(1 - p_i + p_i \frac{n}{N}\right) \equiv \frac{1}{N}\Omega_{3,i}$. In this case the variables change as $n_i^+ \to n_i^+ - 1$ and $n_{i+1}^+ \to n_{i+1}^+ + 1$ if $i > 0$ and $n_1^+ \to n_1^+ + 1$ if $i = 0$.

(4) Finally, we consider a similar case to the previous one but the chosen individual $s_k = -1$ keeps its state. The switching probability is now $\frac{n_i^-}{N}\left(1 - p_i + p_i \frac{N-n}{N}\right) \equiv \frac{1}{N}\Omega_{4,i}$. The changes in the state S_n are $n_i^- \to n_i^- - 1$, $n_{i+1}^- \to n_{i+1}^- + 1$ if $i > 0$ and $n_1^- \to n_1^- + 1$ if $i = 0$.

If time is measured in MCS, the rates (probability per unit time) of the four possible processes are

$$\Omega_{1,i} = n_i^+ \beta_i (1 - n/N), \quad \Omega_{2,i} = n_i^- \beta_i (n/N), \tag{3}$$

$$\Omega_{3,i} = n_i^+ \alpha_i (1 - n/N), \quad \Omega_{4,i} = n_i^- \alpha_i (n/N), \tag{4}$$

[2] Strictly speaking, the aforementioned power-law dependence was reported in [48] for the cumulative inter-event time distribution $C(t)$. One of the authors of that reference (J. Fernández-Gracia, private communication) has confirmed to us that the aforementioned asymptotic time dependence of $\rho(t)$ was also observed, but not displayed.

Please cite this article as: A.F. Peralta, N. Khalil and R. Toral, Ordering dynamics in the voter model with aging, Physica A (2019) 122475, https://doi.org/10.1016/j.physa.2019.122475.

where we have defined the functions $\beta_i(z) = p_i z$ and $\alpha_i(z) = 1 - \beta_i(z)$, thus $\Omega_{1,i} + \Omega_{3,i} = n_i^+$, $\Omega_{2,i} + \Omega_{4,i} = n_i^-$.

This derivation has considered a discrete time process. It is also possible to consider from the beginning a continuous time process in which an agent of age i and state $s = +1$ has a rate $\beta_i(1 - n/N)$ of switching its state and setting its internal age to 0, and a rate $\alpha_i(1 - n/N)$ of increasing its internal age keeping the state; similarly an agent of age i and state $s = -1$ has a rate $\beta_i(n/N)$ of switching its state and setting its internal age to 0, and a rate $\alpha_i(n/N)$ of increasing its internal age and keeping its state.

Following standard techniques [64–66], we could derive a master equation for the probability $P(S_n, t)$ of having state S_n at time t, with the set of rates and changes in the variables explained before. As we restrict ourselves to average values in this paper, we will only obtain the evolution equations for the ensemble average of the fraction of nodes with a given state and age $x_i^\pm = \langle n_i^\pm \rangle / N$, as well as for the total fraction of nodes in the state $+1$, $x = \langle n \rangle / N$. This fraction is related to the magnetization by $m(t) = 2x(t) - 1$. In the all-to-all network considered in this paper, the fraction $x(t)$ is related to the density of active links by $\rho(t) = 2x(t)(1 - x(t))$. The absorbing states correspond to $x = 0, 1$. The time evolution of the average values can be computed as a weighted sum of all the rates that contribute to their variation, the weights being the variation of the regarded variable in that process [66]. Using the standard mean-field approximation [65], which neglects correlations as $\langle n_i^\pm n \rangle \simeq \langle n_i^\pm \rangle \langle n \rangle$, we end up with a closed but infinite system of equations:

$$\frac{dx_i^+}{dt} = -x_i^+ + x_{i-1}^+ \alpha_{i-1}(1 - x), \quad i \geq 1, \tag{5}$$

$$\frac{dx_i^-}{dt} = -x_i^- + x_{i-1}^- \alpha_{i-1}(x), \quad i \geq 1, \tag{6}$$

$$\frac{dx}{dt} = \sum_{i=0}^{\infty} x_i^- \beta_i(x) - \sum_{i=0}^{\infty} x_i^+ \beta_i(1 - x). \tag{7}$$

Similar equations were obtained in Refs. [47,54]. In these equations, variables $x_0^\pm$, whenever they appear, should be expressed in terms of the independent variables,

$$x_0^+ = x - \sum_{i=1}^{\infty} x_i^+, \qquad x_0^- = 1 - x - \sum_{i=1}^{\infty} x_i^-. \tag{8}$$

The explicit time evolution of these variables is

$$\frac{dx_0^+}{dt} = -x_0^+ + \sum_{i=0}^{\infty} x_i^- \beta_i(x), \tag{9}$$

$$\frac{dx_0^-}{dt} = -x_0^- + \sum_{i=0}^{\infty} x_i^+ \beta_i(1 - x). \tag{10}$$

By equating all time derivatives to zero, we can identify the steady-state solutions for the mean-field description. From Eqs. (5), (6), (8) we find

$$x_{i,\mathrm{st}}^+ = \frac{x_{\mathrm{st}}}{f(x_{\mathrm{st}})} \prod_{k=0}^{i-1} \alpha_k(1 - x_{\mathrm{st}}), \qquad x_{i,\mathrm{st}}^- = \frac{1 - x_{\mathrm{st}}}{f(1 - x_{\mathrm{st}})} \prod_{k=0}^{i-1} \alpha_k(x_{\mathrm{st}}), \quad i \geq 0, \tag{11}$$

where

$$f(x) \equiv \sum_{i=0}^{\infty} \prod_{j=0}^{i-1} \alpha_j(1 - x), \tag{12}$$

and the convention $\prod_{j=0}^{-1} \alpha_j \equiv 1$. Obviously, the validity of these relations requires that the series Eq. (12) defining $f(x)$ is convergent. This is certainly not the case for $x = 1$, as $f(x = 1) = \infty$ always. As we will see, another case in which the series might diverge occurs for $p_\infty = 0$, when d'Alembert's criterion does not ensure convergence as $\lim_{i\to\infty} \alpha_i(x) = 1$. Using Eqs. (7), (9), (10) in the steady state, one obtains easily $x_{0,\mathrm{st}}^+ = x_{0,\mathrm{st}}^-$, or

$$\frac{x_{\mathrm{st}}}{f(x_{\mathrm{st}})} = \frac{1 - x_{\mathrm{st}}}{f(1 - x_{\mathrm{st}})}. \tag{13}$$

The solutions to this equation provide the possible steady-state values of $x_{\mathrm{st}} = \langle n \rangle / N$ and those values of x_{st} determine the other quantities, through Eqs. (11). Note that $x_{\mathrm{st}} = 1/2$ is always a trivial solution that corresponds to a symmetric steady state, with the same mean number of nodes with a given age having opposite states $x_{i,\mathrm{st}}^+ = x_{i,\mathrm{st}}^-$ for $i \geq 0$. In any case, the steady-state solutions describe situations where $x_{i,\mathrm{st}}^\pm$ are decreasing functions of the age. Note also that the absorbing states $x_{\mathrm{st}} = 0, 1$ are always steady state solutions of the dynamics, and indeed they satisfy Eq. (13) as $f(x \to 1) \to \infty$ and $f(x \to 0) \to$ constant.

Please cite this article as: A.F. Peralta, N. Khalil and R. Toral, Ordering dynamics in the voter model with aging, Physica A (2019) 122475, https://doi.org/10.1016/j.physa.2019.122475.

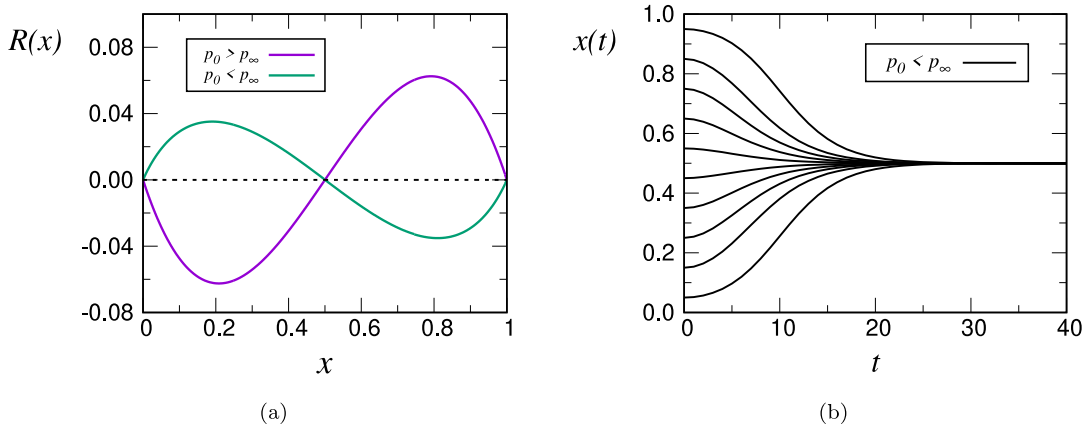

Fig. 1. In the left panel we show the function $R(x) \equiv \frac{1-x}{f(1-x)} - \frac{x}{f(x)}$, with $f(x)$ defined in Eq. (12). The sign of $R(x)$ determines the stability of the fixed points of the dynamical variable x, the fraction of nodes in the state $+1$ (see the main text). This plot uses the rational form of the activation probabilities as given by Eq. (1) for the cases: (i) aging $p_0 = 0.9 > p_\infty = 0.1$ and $c = 1$, purple line, and (ii) anti-aging, $p_0 = 0.1 < p_\infty = 0.9$ and $c = 1$, green line. In case (i), the $x = 1/2$ state is unstable and the dynamics leads to any of the two stable fixed points, $x = 0$, $x = 1$. In case (ii) the situation is reversed and the state $x = 1/2$ is the stable one, while $x = 0$, $x = 1$ are unstable. The right panel shows trajectories $x(t)$ coming from numerical simulations in the anti-aging case, $p_0 = 0.5 < p_\infty = 1$ and $c = 1$, with different initial conditions $x(0)$ and $N = 10^5$ agents, averages were performed over 10^2 trajectories. All these averaged trajectories end up in the stable fixed point $x = 1/2$. In this and subsequent figures, the numerical simulations use the rules spelled out in the definition of the model, Section 2.

For the particular case $p_i = p, \forall i$, we obtain the function $f(x) = 1/(p(1-x))$. Eq. (13) is satisfied for any $x_{\rm st}$ and, in fact, it can be shown that Eq. (7) becomes $\frac{dx}{dt} = 0$ and, hence, $x_{\rm st} = x(0)$. This is the behavior of the non-aging voter model in the thermodynamic limit that was described before. If $x_{\rm st} \neq 0, 1$, the distribution of ages in this steady state follows a geometric distribution: $x^+_{i,\rm st} = p x_{\rm st}(1-x_{\rm st})(1-p(1-x_{\rm st}))^i$ and $x^-_{i,\rm st} = p x_{\rm st}(1-x_{\rm st})(1-p x_{\rm st})^i$. For $x_{\rm st} = 0, 1$, see Section 5.

For the activation probabilities corresponding to a rational function of the age, i.e. Eq. (1), one finds[3]

$$f(x) = 1 + (1 - p_0(1-x))\ {}_2F_1\left[1, 1 + c\frac{1-p_0(1-x)}{1-p_\infty(1-x)}; 1+c; 1-p_\infty(1-x)\right], \tag{14}$$

where ${}_2F_1[\alpha, \beta; \gamma; x]$ is the Gauss hypergeometric function. This function, and hence the series Eq. (12), is always convergent for $p_\infty(1-x) > 0$. If $x = 1$, we already know that the series is divergent. If $p_\infty = 0$, the series diverges whenever $x \geq 1 - 1/(cp_0)$. Although these divergences may be problematic in the case $p_\infty = 0$, one can still study Eq. (13) as a limit $p_\infty \to 0$ or, alternatively regularize the sum Eq. (12) with a cut-off $\sum_{i=0}^{M}(\dots)$ and study the dependence with M.[4] We checked that the predicted behavior of the fixed points of Eq. (13) in all cases is correct. In Fig. 1(a) we plot $R(x) \equiv \frac{1-x}{f(1-x)} - \frac{x}{f(x)}$ in a case of aging $p_0 > p_\infty$ and anti-aging $p_0 < p_\infty$. We find in both cases that $R(x_{\rm st}) = 0$ provides the three mentioned fixed points, $x_{\rm st} = 0,\ 1/2,\ 1$. We also hypothesize [67] that the sign of $R(x)$ determines the stability and direction of movement of x, $\frac{dx}{dt}$, thus for aging we expect the symmetric solution $x_{\rm st} = 1/2$ to be unstable and the absorbing states $x_{\rm st} = 0, 1$ stable, and the other way around for anti-aging [68]. The stability of the $x_{\rm st} = 1/2$ state is shown in Fig. 1(b). The time-dependence and ordering dynamics depending on the form of p_i is studied in detail in the next section.

5. Ordering dynamics

It is clear from the rules of the process that the absorbing states $x(t) = 0$ and $x(t) = 1$ must be solutions of the dynamical equations in all cases, whatever the particular form of p_i. We now discuss these solutions. For the sake of concreteness we consider only the $x = 0$ absorbing state, but an equivalent analysis could be performed at $x = 1$ as well. Consider, then, that the system is at $x = 0$ at time $t = 0$ with all internal ages set to 0. As there are no nodes in the $+1$ state, the herding mechanism implies that a selected node can never switch state to $+1$ and will remain in the -1 state, hence increasing its internal age in one unit according to the rules of the model. Therefore we have $x_i^{+(0)}(t) = 0$, $x^{(0)}(t) = 0$, and thus Eq. (10) reduces to $\frac{dx_0^{-(0)}}{dt} = -x_0^{-(0)}$, or $x_0^{-(0)}(t) = e^{-t}$, where the superscript (0) indicates that those

[3] Simpler expressions are obtained if c is an integer number, e.g. $f(x) = [p_\infty(1-x)]^{-\frac{1-p_0(1-x)}{1-p_\infty(1-x)}}$, if $c = 1$.

[4] In some cases this limit is non-trivial and must be performed carefully. Specially when p_i decays very fast as in the exponential example. A possibility is to consider $M(t)$ as time dependent and a phenomenological reasoning based on imposing convergence of $f(x) \sim M(t)\prod_k^t \alpha_k(1-x)$ with $t \to \infty$ suggests $M(t) \sim \left[\prod_k^t (1 - p_k x(0))\right]^{-1}$. This is similar to imposing $\frac{dx_i^{\pm}}{dt} = 0$ only for $i < t$ lower than the simulation time t.

Please cite this article as: A.F. Peralta, N. Khalil and R. Toral, Ordering dynamics in the voter model with aging, Physica A (2019) 122475, https://doi.org/10.1016/j.physa.2019.122475.

values are valid at the absorbing state $x = 0$. The solution of Eqs. (6) with $x = 0$ (implying $\alpha_j(0) = 1$) and the above mentioned initial conditions can be readily found as

$$x_i^{-(0)}(t) = e^{-t}\frac{t^i}{i!}, \quad i \geq 0, \tag{15}$$

which indicates that the distribution of internal ages in the population follows a Poisson distribution with $\langle i \rangle = \sigma_i^2 = t$. We now study the stability of this solution.

We linearize Eqs. (5), (9) around the solution $x_i^{\pm(0)}$ at the absorbing state:

$$\frac{dx_i^+}{dt} = -x_i^+ + x_{i-1}^+(1 - p_{i-1}), \quad i \geq 1, \tag{16}$$

$$\frac{dx_0^+}{dt} = -x_0^+ + x\sum_{i=0}^{\infty} p_i x_i^{-(0)} = -x_0^+ + x\sum_{i=0}^{\infty} p_i e^{-t}\frac{t^i}{i!}. \tag{17}$$

The solution of Eq. (16) with the initial condition $x_i^+(0) = 0$, $i \geq 1$, is

$$x_i^+(t) = \prod_{k=0}^{i-1}(1 - p_k)\int_0^t \frac{(t-s)^{i-1}}{(i-1)!}e^{s-t}x_0^+(s)ds, \quad i \geq 1. \tag{18}$$

Imposing $x(t) = x_0^+(t) + \sum_{i=1}^{\infty} x_i^+(t)$, and replacing in Eq. (17) we obtain

$$x(t) = x_0^+(t) + \int_0^t G(t-s)x_0^+(s)ds, \tag{19}$$

$$\frac{dx_0^+}{dt} = -x_0^+ + L(t)\left(x_0^+ + \int_0^t G(t-s)x_0^+(s)ds\right), \tag{20}$$

with

$$G(t) = e^{-t}\sum_{i=0}^{\infty}\frac{t^i}{i!}\prod_{k=0}^{i}(1 - p_k), \tag{21}$$

$$L(t) = e^{-t}\sum_{i=0}^{\infty} p_i\frac{t^i}{i!}. \tag{22}$$

The integro-differential equation (20) has to be solved with the initial condition $x_0^+(0) = x(0)$. Here $G(t)$ can be interpreted as the memory kernel of the dynamics, which reflects the importance of the state occurred a time t ago in the determination of the next state.

A simple case in which the linearized equations (19), (20) can be solved explicitly is $p_i = p$, constant. In this case we have $L(t) = p$ and $G(z) = (1-p)e^{-pz}$, which after a tedious but straightforward calculation,[5] leads to $x_0^+(t) = x(0)(p + (1-p)e^{-t})$ and $x(t) = x(0)$, the well known solution of the voter model in the thermodynamic limit,[6] $N \to \infty$.

As it follows from Eqs. (19), (20) that $x'(0) \equiv \left.\frac{dx}{dt}\right|_{t=0} = 0$, the stability of $x(t)$ requires to study the sign of $x''(0) \equiv \left.\frac{d^2x}{dt^2}\right|_{t=0}$, which after a simple calculation turns out to be $x''(0) = p_0(p_1 - p_0)$. Therefore, at this level, we obtain that in the anti-aging case, $p_0 < p_1$, the absorbing solution $x = 0$ is unstable, while in the aging case, $p_0 > p_1$, the absorbing solution is stable, as suggested at the end of the previous section. Since for both functional forms Eqs. (1), (2) in the anti-aging case there are no other solutions than $x_{st} = 1/2$, we predict that the final state of the dynamics is that of coexistence of states. This is indeed observed in the numerical simulations, as shown in Fig. 1(b). We conclude, then, that the anti-aging version of the model, where the activation probability p_i is an increasing function of age i, always leads to a steady-state solution of coexistence of states and lack of consensus[7] [68]. The stability analysis can be also explained qualitatively. Initially all nodes have zero age and thus they evolve as the traditional voter model, this justifies $x'(0) = 0$. After a small time period some nodes change state and thus are younger than the rest, the proportion of young ± 1 being $1/2$ in order to keep $x(t) \approx x(0)$. In the case of aging, young nodes change state easier ($p_0 > p_1$) and thus copy the state of the older ones following the proportion $x(0)$ causing $x(t) \to 1$ if $x(0) > 1/2$ and $x(t) \to 0$ if $x(0) < 1/2$. For anti-aging, old nodes change easier ($p_0 < p_1$) thus the symmetric proportion $1/2$ of the young nodes tends to remain causing $x(t) \to 1/2$.

[5] A possibility is to use the Laplace transform in Eqs. (19), (20).

[6] Note here that $x_0^+(\infty) = px(0)$ in apparent contradiction to the result of Section 4 $x_{0,st}^+ = px_{st}(1 - x_{st})$. But this is a product of the linearization in Eqs. (19), (20).

[7] This conclusion, again, is valid in the thermodynamic limit. For a finite system, there will always be a fluctuation, whose likelihood decreases with system size, that will lead to a consensus state.

Please cite this article as: A.F. Peralta, N. Khalil and R. Toral, Ordering dynamics in the voter model with aging, Physica A (2019) 122475, https://doi.org/10.1016/j.physa.2019.122475.

To study in full detail the return to the absorbing state of the variable $x(t)$, we would need to solve the linearized equations (19), (20). Although it does not seem to be possible to obtain their full time dependence analytically,[8] simple arguments allow us to obtain the asymptotic behaviors for large t. All we need for this purpose is the asymptotic expressions of $G(t)$ and $L(t)$. We split the discussion in the cases $p_\infty = 0$ and $p_\infty > 0$, as the difference is of crucial importance.

5.1. A rational function activation probability, Eq. (1), with $p_\infty = 0$

This case includes the one studied in [48] where the activation probability decayed as $p_i \sim b/i$. With our explicit expression, Eq. (1), the calculation of Appendix A.1 leads to an asymptotic behavior valid for $p_0 < 1$,

$$G(t) \sim \frac{\Gamma(c)}{\Gamma(c(1-p_0))} t^{-b}, \tag{23}$$

$$L(t) \sim b\, t^{-1}, \quad b = cp_0, \tag{24}$$

where $\Gamma(z)$ is Euler's Gamma function. Note that the memory kernel $G(t)$ decays asymptotically as a power law, thus the system exhibits long memory effects.

Assuming power-law dependences as $x_0^+(t) \sim t^{-\alpha}$, $x(t) \sim t^{-\beta}$ and that the integral in Eq. (20) can be approximated as $\int_0^t G(t-s)x_0^+(s)ds \sim AG(t) \sim t^{-b}$, with $A = \int_0^\infty x_0^+(s)ds$, which is justified if the time evolution of $x_0^+(t)$ is slower than that of $G(t)$, we obtain consistently $\alpha = b+1$. Finally, using this value with Eq. (19) we get $\beta = b$. This proves that the density of nodes in the + state and, consequently, the density of active links go to zero as $x(t) \sim \rho(t) \sim t^{-b}$, explaining the numerical fits of Ref. [48], this being one of the main results of our paper.

To further check the previous predictions, we plot in Fig. 2 the results coming from numerical simulations for $x_0^+(t)$ and $x(t)$ for different cases of p_0 and c. As is apparent, the figures confirm the validity of the asymptotic expansion $x(t) \sim t^{-b}$ and $x_0^+(t) \sim t^{-b-1}$, as derived theoretically with an exponent $b = p_0 c$ that corresponds to the asymptotic law $p_i \sim b/i$. Besides the asymptotic slope, we also plot in the figures the values of $x(t)$ and $x_0^+(t)$ obtained from the numerical solution of Eqs. (19), (20) using a suitable integration algorithm described in Ref. [70].

The discussion so far has assumed hat $p_0 < 1$. If $p_0 = 1$, $G(t) = 0$ and a direct integration of Eqs. (19), (20) leads to an initial decay $x(t) \sim e^{-t^2/(2(1+c))}$, followed by an intermediate regime $x(t) \sim t^b e^{-t}$. In the numerical simulations we observe that this is followed by a crossover to the same asymptotic power-law behavior $x(t) \sim t^{-b}$, see panels (b) and (d) of Fig. 2. The reason why the integro-differential equations (19), (20) do not capture this crossover is because they are linearized. The solution of the full set of equations Eqs. (5)–(7) can be written $x(t) = x(0)h_1(t) + x(0)^2 h_2(t) + \ldots$ with the different orders of the initial condition $x(0)$. Linearizing, we were able to find the first term $h_1(t)$. For $p_0 \neq 1$ this first term is a power-law and it prevails over the rest for all times. For $p_0 = 1$ it decays exponentially and, apparently, the second order term $h_2(t) \sim t^{-b}$ is a power-law. Thus, for sufficiently large times $t > t^*$ it can happen that $x(0)h_1(t) < x(0)^2 h_2(t)$. In order to understand the role of p_0 in the accuracy of the approximate solution, we can compute the scaling of the relative error of the linearized solution as $\varepsilon \equiv (x_{\text{linear}}(t) - x_{\text{exact}}(t))/x_{\text{linear}}(t)$ as we approach $p_0 \to 1$. We know that asymptotically $x(0)h_1(t) \sim AG(t)$, such that when $p_0 \to 1$ it is $h_1(t) \sim \mathcal{C}_1(1-p_0)t^{-b}$ and we derived here, from the numerical results, that $h_2(t) \sim \mathcal{C}_2 t^{-b}$, where $\mathcal{C}_{1,2}$ are non-zero for $p_0 \to 1$. Thus, the relative error scales as $\varepsilon \sim \frac{x(0)}{1-p_0}\frac{\mathcal{C}_2}{\mathcal{C}_1}$. This is directly proportionally to $x(0)$ and inversely to $1-p_0$. For $p_0 = 1$ the error tends to infinity, reflecting that the approximate solution does not capture correctly the time dependence.

We now consider the age distribution $x_i^+(t)$ for $i \geq 1$. The kernel $\frac{(t-s)^{i-1}}{(i-1)!}e^{s-t}$ inside the integral of Eq. (18) is a Poisson distribution with $\langle i-1\rangle = \sigma_{i-1}^2 = t-s$, which localizes the integral of $x_0^+(s)$ in a window of position and width determined by i. This tells us that in order to find the qualitative shape of the age distribution $x_i^+(t)$ for $i \sim t \gg 1$, we can replace the early dynamics approximate solution $x_0^+(s)$ inside the integral at Eq. (18) by $x(0)e^{-(1-p_0)s}$ and $\prod_{k=0}^{i-1}(1-p_k)$ by its asymptotic expansion form $\frac{\Gamma(c)}{\Gamma(c(1-p_0))}i^{-b}$ for $i \gg 1$:

$$x_{i\gg 1}^+(t) \simeq \frac{x_0^+(0)}{t^b}\frac{\Gamma(c)}{\Gamma(c(1-p_0))}\int_0^t \frac{(t-s)^{i-1}}{(i-1)!}e^{p_0 s - t}ds. \tag{25}$$

This is essentially a function localized around $i \sim t$ whose amplitude decreases as $1/t^b$. This feature of the distribution of ages is analyzed in Fig. 3. For $i \gtrsim 1$, however, the major contribution to the integral at Eq. (18) comes from the region $s \sim t \gg 1$ and we can use the asymptotic expression $x_0^+(s) = As^{-(b+1)}$ as a constant inside the integral

$$x_{i\gtrsim 1}^+(t) \simeq B_i t^{-(b+1)}, \quad B_i \equiv A\prod_{k=0}^{i-1}(1-p_k), \tag{26}$$

whose validity is checked in Fig. 3.

[8] It is possible to try a power-series expansion $x(t) = \sum_{k=0}^\infty a_k t^k$ and $x_0^+(t) = \sum_{k=0}^\infty b_k t^k$ and obtain recurrence relations for the coefficients a_k, b_k, see [69], but we have not been able to sum analytically the resulting series.

Please cite this article as: A.F. Peralta, N. Khalil and R. Toral, Ordering dynamics in the voter model with aging, Physica A (2019) 122475, https://doi.org/10.1016/j.physa.2019.122475.

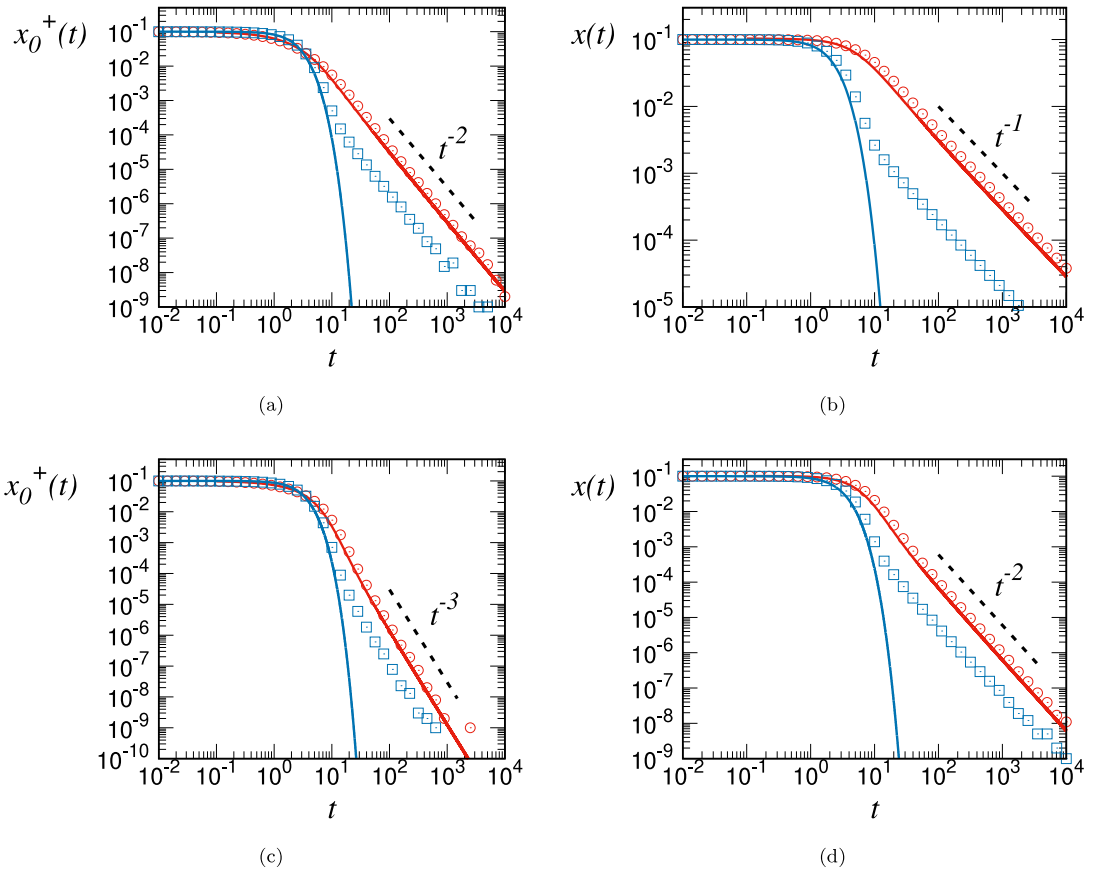

Fig. 2. Time evolution of the fraction $x(t)$ of individuals in the state $+1$, and the fraction $x_0^+(t)$ of individuals in the state $+1$ having internal age equal to 0. These plots use the rational form of the activation probabilities p_i as given by Eq. (1) in the case of aging, $p_\infty = 0$, and with different values of p_0 and c. In all cases the initial conditions are $x(0) = x_0^+(0) = 0.1$. Top panels correspond to $p_0 = 1/2$, $c = 2$ (red circles and red line), and $p_0 = 1$, $c = 1$ (blue squares and blue line), with the same value of $b \equiv p_0 c = 1$ in both cases. Bottom panels correspond to $p_0 = 2/3$, $c = 3$ (red circles and red line), and $p_0 = 1$, $c = 2$ (blue squares and blue line) and the common value $b \equiv p_0 c = 2$. Points are results from numerical simulations with $N = 10^5$ averaged over 10^4 trajectories while lines come from the numerical integration of Eqs. (19), (20). The plots provide evidence of the asymptotic laws $x(t) \sim t^{-b}$ and $x_0^+(t) \sim t^{-b-1}$. The failure of the numerical integration to reproduce the asymptotic results for $p_0 = 1$ is discussed in the main text.

5.2. A rational function activation probability, Eq. (1), with $p_\infty > 0$

In this case the activation probability starts at p_0 and evolves to a non-null value p_∞. This is qualitatively similar to the case studied in [47], although in that reference the final value p_∞ was reached after a finite number of aging steps, but we do not expect this to be a significant difference.

As shown in Appendix A.1, $L(t)$ tends to a non-null asymptotic value $L(t \to \infty) = p_\infty$ while $G(t)$ decays exponentially, thus memory effects extend over a limited time given by $1/p_\infty$:

$$G(t) \sim e^{-p_\infty t} t^{-b}, \quad b = c\frac{p_0 - p_\infty}{1 - p_\infty}, \tag{27}$$

$$L(t) \sim p_\infty. \tag{28}$$

If we replace $L(t)$ by this constant value p_∞ in Eq. (20) we can use the Laplace transform $\hat{x}_0^+(s)$ of $x_0^+(t)$ to find the explicit solution:

$$\hat{x}_0^+(s) = \frac{x(0)}{s + 1 - p_\infty(1 + \hat{G}(s))} \equiv \frac{x(0)}{\hat{F}(s)}, \tag{29}$$

and from Eq. (19) we get the Laplace transform $\hat{x}(s)$ of $x(t)$:

$$\hat{x}(s) = \frac{1 + \hat{G}(s)}{\hat{F}(s)} x(0). \tag{30}$$

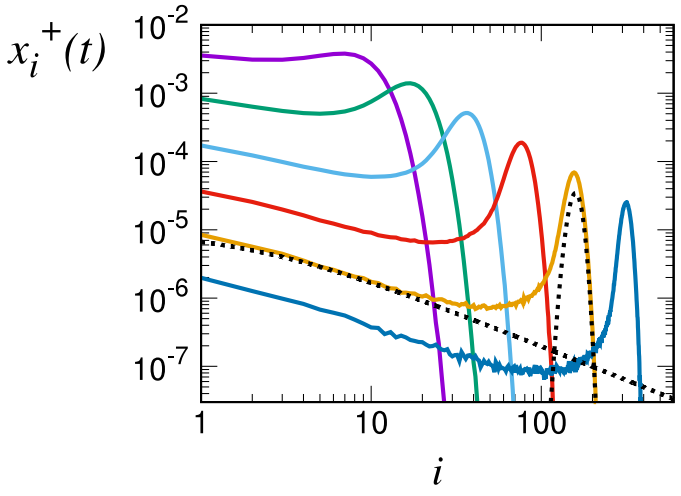

Fig. 3. Time evolution of the density $x_i^+(t)$ of nodes in state $+$ with age i. This plot uses the rational form of the activation probabilities p_i as given by Eq. (1) in the case of aging with $p_\infty = 0$, $p_0 = 1/2$ and $c = 2$. The initial condition is $x_i^+(0) = 0.1\delta_{i,0}$. Colored lines are the results of numerical simulations with $N = 10^5$ nodes averaged over 10^4 trajectories. $x_i^+(t)$ is showed as a function of i for different snapshots $t = 10, 20, 40, 80, 160, 320$ (from top to bottom at $i = 1$) in a log–log scale. For $t = 160$ the dashed black lines are the asymptotic approximations Eq. (25) for $i \gg 1$ and Eq. (26) for $i \gtrsim 1$.

Note that, due to the asymptotic behavior of $G(t)$, Eq. (27), the Laplace transform $\hat{G}(s)$ does not converge for $s < -p_\infty$. It turns out that $\hat{F}(s)$ has a zero located at $s = s_1$. Hence, inverting the Laplace transform we find the asymptotic behavior $x_0^+(t) \sim x(t) \sim e^{s_1 t}$. The exact value of s_1 has to be obtained solving numerically $\hat{F}(s_1) = 0$ and it is found to depend non-trivially on the parameters of the model, see Fig. 4(a). As it is shown in this figure, we find $s_1 < 0$ for $p_0 > p_\infty$ (aging) and $s_1 > 0$ for $p_0 < p_\infty$ (anti-aging), thus the asymptotic behavior is in accordance to the linear stability analysis of Eqs. (19), (20) performed before. There are two cases where $s_1 = 0$: (i) for $p_0 = p_\infty$ which corresponds to the non-aging voter model with $x(t) = x(0)$, and (ii) for $p_\infty = 0$ where the time dependence changes from being exponential to a power-law $x(t) \sim t^{-\beta}$ as explained in the previous Section 5.1. The case that concern us in this section is $0 < p_\infty < p_0$, where we have $s_1 \sim -p_\infty$ for small p_∞ and as p_∞ approaches p_0, s_1 increases until $s_1 = 0$. This analysis is in accordance with the counterintuitive result of Ref. [47], and it shows that the consensus state is a stable fixed point of the dynamics in the case of an activation probability that decays to a non-zero value p_∞.

We have checked in Fig. 5 the predicted asymptotic behavior in the particular case $p_\infty = 0.1$, $p_0 = 0.5$, $c = 1$. The theory predicts an exponential decay of the fraction $x(t)$ of individuals in the state $+1$, and the fraction $x_0^+(t)$ of individuals in the state $+1$ having internal age equal to 0, $x_0^+(t) \sim x(t) \sim e^{s_1 t}$, with $s_1 = -0.0982$ which matches perfectly compared to numerical simulation and also compared to the numerical solution of Eqs. (19), (20). In the same figure we also show the special problematic case $p_0 = 1$, with the same other parameters. In this case $G(t) = 0$ and thus, according to Eqs. (19), (20), the solution is initially an exponential function as $x(t) \approx e^{-\frac{1-p_\infty}{2(1-c)}t^2}$ followed by the regime $x(t) \approx e^{-(1-p_\infty)t} t^{p_0 c}$. This behavior is correct in the early states of the dynamics but after it there is a crossover to a slower exponential decay $x(t) \sim e^{s_1^* t}$. We expect this effect to be also a result of linearization, where in $x(t) = x(0)h_1(t) + x(0)^2 h_2(t) + \ldots$, $h_2(t)$ is slower than $h_1(t)$ which is the result that we obtained. Thus for a large enough time $t > t^*$ it can happen that $x(0)h_1(t) < x(0)^2 h_2(t)$.

Note that $x(t) \sim e^{st}$ is the natural result of the linearization of a Markovian type of evolution equation $\frac{dx}{dt} \propto R(x)$. This implies that in this case one can define an effective Markovian process that shows the same type of dynamical behavior as the non-Markovian model. This is not the case for the activation probabilities studied in Sections 5.1 and 5.3, and this explains why $R(x) \equiv \frac{1-x}{f(1-x)} - \frac{x}{f(x)}$, defined at the end Section 4, shows divergence problems for those cases.

5.3. An exponential function activation probability, Eq. (2), with $p_\infty = 0$

Using this exponential form of the activation probability we find in Appendix A.2 the asymptotic behavior for large t

$$G(t) \sim (p_0; \lambda)_\infty , \tag{31}$$

$$L(t) = p_0 e^{-(1-\lambda)t}, \tag{32}$$

where $(a; b)_i \equiv \prod_{k=0}^{i-1}(1 - ab^k)$ is the q-Pochhammer symbol [71]. Note the remarkable property that $G(t \to \infty) \to$ constant > 0 which is something that we did not observe in the case of a rational function activation probability p_i. This indicates that the memory extends over the whole past history of states. As explained in Appendix B, we can solve Eqs.

Please cite this article as: A.F. Peralta, N. Khalil and R. Toral, Ordering dynamics in the voter model with aging, Physica A (2019) 122475, https://doi.org/10.1016/j.physa.2019.122475.

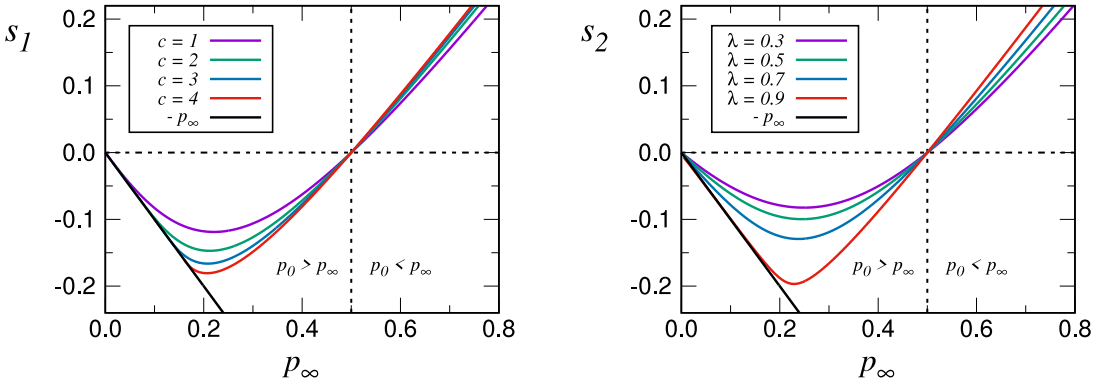

Fig. 4. Roots of the function $\hat{F}(s) = s + 1 - p_\infty(1 + \hat{G}(s))$, i.e. the solutions of $\hat{F}(s) = 0$, that appears in the denominator of the Laplace transforms $\hat{x}(s)$ and $\hat{x}_0^+(s)$ of, respectively, the fraction $x(t)$ of individuals in the state $+1$, and the fraction $x_0^+(t)$ of individuals in the state $+1$ having internal age equal to 0. The roots are plotted as a function of p_∞. The left panel uses the rational form of the activation probabilities p_i as given by Eq. (1) with fixed $p_0 = 1/2$ and for different values of $c = 1, 2, 3, 4$. The right panel uses instead the exponential form of the activation probabilities p_i as given by Eq. (2) for different values of $\lambda = 0.3, 0.5, 0.7, 0.9$. The explicit forms of the Laplace transform $\hat{G}(s)$ in both cases are given in Appendix A. For the rational form, the roots tend to 0 as $s = -p_\infty$, as indicated by the straight solid black line. The vertical lines at $p_\infty = 1/2$ separate the aging, $p_0 > p_\infty$, and the anti-aging, $p_0 < p_\infty$, cases. It is clear that the roots are negative for aging and positive for anti-aging. Hence, the asymptotic behavior $x_0^+(t) \sim x(t) \sim e^{st}$, being $s = s_1$ or $s = s_2$ for each case, is in accordance with the linear stability analysis, see the main text for details.

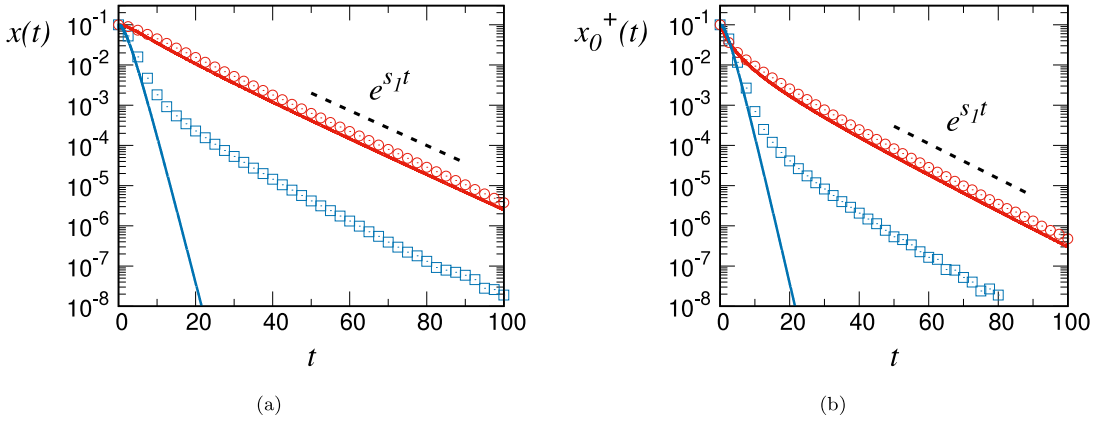

Fig. 5. Time evolution of the fraction $x(t)$ of individuals in the state $+1$, and the fraction $x_0^+(t)$ of individuals in the state $+1$ having internal age equal to 0. These plots use the rational form of the activation probabilities p_i as given by Eq. (1) in the case of aging, but at variance with the results displayed in Fig. 2, the activation probability does not decay to $p_\infty = 0$ but to a finite value $p_\infty = 0.1$. As it can be seen from these figures, the fraction $x(t)$ tends to $x(t) = 0$ (the consensus state) as an exponential function of time instead of a power-law observed in Fig. 2. Red circles and red lines correspond to $p_0 = 1/2$, $c = 1$, while blue squares and blue lines correspond to $p_0 = 1$, $c = 1$. The points are the result of numerical simulations with $N = 10^5$ averaged over 10^4 trajectories, while solid lines are the numerical integration of Eqs. (19), (20). The initial condition is $x(0) = x_0^+(0) = 0.1$. The dashed lines indicate the exponential decay $x(t) \sim x_0^+(t) \sim e^{s_1 t}$ with $s_1 = -0.0982\ldots$ predicted by the theory, see Section 5.2.

(19), (20) in this case replacing Eqs. (31), (32). Approximately, we have the exponential decay of the fraction $x_0^+(t)$ of individuals in the state $+1$ having internal age equal to 0, $x_0^+(t) \approx x_0(0)c_2 e^{-(1-\lambda)t}$, while the fraction $x(t)$ of individuals in the state $+1$ decays exponentially until it reaches a constant value $x(\infty) \approx x(0)c_2\lambda/p_0$ that depends on the initial condition $x(0)$. Here c_2 is a constant that depends on p_0 and λ in an intricate way, see Appendix B.

In summary, the system does not order in this case. We can deduce that this will be the case as long as $G(\infty) = \prod_{k=0}^{\infty}(1-p_k) > 0$ (unlimited memory) or, equivalently, if $\sum_{k=0}^{\infty} p_k$ converges. Obviously for $p_\infty \neq 0$ this is never the case, while for $p_\infty = 0$ if p_k decays faster than $p_k \sim 1/k$ the system does no order, but it does order if p_k decays slower than $p_k \sim 1/k$. The case $p_k \sim 1/k$ is a borderline value, where the system orders very slowly as a power-law as explored in Section 5.1. It seems, then, that the reaching of consensus induced by aging depends crucially on the specific functional dependence of the activation probability p_i.

In Fig. 6(a) we show that, in accordance with the theoretical results, the fraction $x(t)$ of individuals in the state $+1$ reaches a constant value, while Fig. 6(b) confirms that the fraction $x_0^+(t)$ of individuals in the state $+1$ having

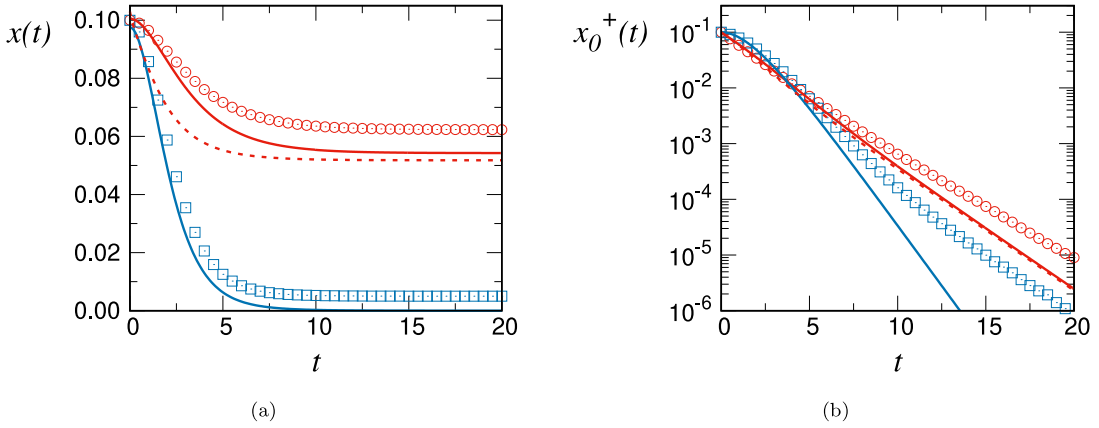

Fig. 6. Time evolution of the fraction $x(t)$ of individuals in the state $+1$, and the fraction $x_0^+(t)$ of individuals in the state $+1$ having internal age equal to 0. The plots use the exponential form of the activation probabilities p_i as given by Eq. (2) with $p_\infty = 0$ and $\lambda = 1/2$, i.e. a situation of aging. Red circles and red lines are for $p_0 = 1/2$, while blue squares and blue lines for $p_0 = 1$. Points are results from numerical simulations with $N = 10^5$ averaged over 10^4 trajectories, while lines are the numerical integration of Eqs. (19), (20). The initial conditions are $x(0) = x_0^+(0) = 0.1$. The dashed lines are the approximate solution of Appendix B. It can be seen that $x(t)$ does not decay to $x(\infty) = 0$ but to a finite value $x(\infty)$, and hence the system does not reach the consensus state, at variance to what happened when the activation probabilities were described by a rational decay to $p_\infty = 0$, as shown in Fig. 2.

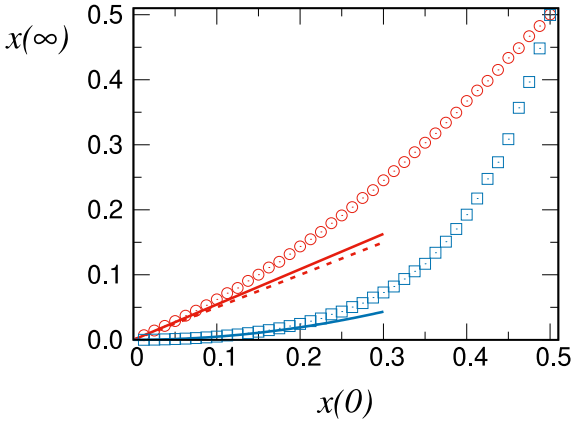

Fig. 7. Stationary value $x(\infty)$ of the fraction of individuals in the state $+1$ observed in Fig. 6 as a function of the initial condition $x(0)$, for the same values of the parameters: $p_\infty = 0$, $\lambda = 1/2$ and $p_0 = 1/2$ (red circles), $p_0 = 1$ (blue squares). The red solid line is the result of the numerical integration of the linearized Eqs. (19), (20), while the dashed line is the approximation of Appendix B, i.e. $x(\infty) \approx c_2\lambda/p_0 x(0)$. The $p_0 = 1$ case confirms the predicted dependence $x(\infty) \propto x(0)^2$, the solid blue line being a quadratic fit of the numerical points for $x(0) \ll 1$.

internal age equal to 0 decreases exponentially. We have considered in these figures the values $(p_0, \lambda) = (1/2, 1/2)$ and $(p_0, \lambda) = (1, 1/2)$. In the latter case, and similarly to what was discussed before, there is a failure of the linearization. While the theory predicts that the system orders exponentially, the numerical simulations indicate an initial exponential decay that crosses over to a constant value $x(\infty) \neq 0$, which is smaller than the corresponding one in the case $p_0 < 1$. According to this argument $x(t) = x(0)h_1(t) + x(0)^2 h_2(t) + \ldots$, $h_1(\infty) = 0$ and $h_2(\infty) \neq 0$ and the fixed point value is expected to scale instead as $x(\infty) \propto x(0)^2$, for $x(0) \ll 1$.

In Fig. 7 we plot the dependence of $x(\infty)$ with the initial value $x(0)$ confirming both the linear prediction $x(\infty) \approx c_2\lambda/p_0 x(0)$ valid for $p_0 < 1$ and the quadratic dependence $x(\infty) \propto x(0)^2$ valid for $p_0 = 1$.

5.4. An exponential function activation probability, Eq. (2), with $p_\infty > 0$

Using this exponential form of the activation probability we find in Appendix A.2 the asymptotic expressions

$$G(t) \sim (1 - p_\infty) \left(\frac{p_0 - p_\infty}{1 - p_\infty}; \lambda \right)_\infty e^{-p_\infty t}, \tag{33}$$

$$L(t) \sim p_\infty. \tag{34}$$

Please cite this article as: A.F. Peralta, N. Khalil and R. Toral, Ordering dynamics in the voter model with aging, Physica A (2019) 122475, https://doi.org/10.1016/j.physa.2019.122475.

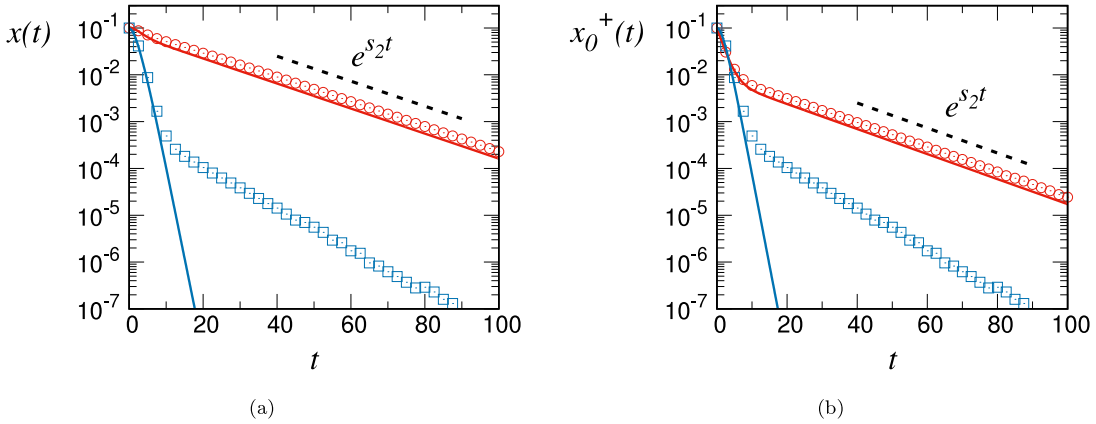

Fig. 8. Time evolution of the fraction $x(t)$ of individuals in the state $+1$, and the fraction $x_0^+(t)$ of individuals in the state $+1$ having internal age equal to 0. The plots use the exponential form of the activation probabilities p_i as given by Eq. (2) with $p_\infty = 0.1$ and $\lambda = 1/2$. Red circles and red lines correspond to $p_0 = 1/2$, $\lambda = 1/2$, while blue squares and blue lines to $p_0 = 1$, a situation of aging in both cases. Points are results from numerical simulations with $N = 10^5$ averaged over 10^4 trajectories, while lines are the numerical integration of Eqs. (19), (20). As $x(t \to \infty) = 0$, the system reaches the consensus state, similarly to the case displayed in Fig. 5 corresponding to an activation probability which is a rational function of the age. The dashed lines indicate the exponential decay $x(t) \sim x_0^+(t) \sim e^{s_2 t}$ with $s_2 = -0.0616\ldots$, predicted by the theory, see Section 5.4.

Thus, this case is similar to the one studied in Section 5.2 where $G(t)$ decays exponentially and $L(t)$ goes to a constant. Following the procedure of that subsection we predict an exponential decay of both the fraction $x(t)$ of individuals in the state $+1$, and the fraction $x_0^+(t)$ of individuals in the state $+1$ having internal age equal to 0, as $x(t) \sim x_0^+(t) \sim e^{s_2 t}$. The parameter of the exponential decay s_2 is obtained as the root of the function $\hat{F}(s) = s + 1 - p_\infty(1 + \hat{G}(s))$, using the Laplace transform $\hat{G}(s)$ of $G(t)$ as given in Eq. (A.13). We plot in Fig. 4(b) the dependence of s_2 with p_0, finding the same phenomenology than in the case of a rational function activation probability discussed in Section 5.2, i.e. $s_2 < 0$ for $p_0 > p_\infty$ (exponential decay to the stable fixed point $x = 0$ in the aging case); $s_2 > 0$ for $p_0 < p_\infty$ (instability of the $x = 0$ consensus state in the anti-aging regime). When $s_2 = 0$ the exponential decay is not valid. This occurs for $p_0 = p_\infty$, corresponding to the non-aging voter model for which $x(t) = x(0)$, and for $p_\infty = 0$ where $x(t)$ decays to a constant value, as it was shown in Section 5.3.

In Fig. 8 we compare the results of numerical simulations of $x(t)$ with the numerical integration of Eqs. (19), (20) and the predicted asymptotic behavior $x(t) \sim x_0^+(t) \sim e^{s_2 t}$, using $p_\infty = 0.1$, $\lambda = 0.5$ and the two values $p_0 = 0.5$ and $p_0 = 1$. For $p_0 = 0.5$ the theory predicts $s_2 = -0.0616\ldots$ which is in good agreement with the simulation. The case $p_0 = 1$ is again singular as the linear approximation fails to reproduce the long term dynamics. In the linear theory we have $G(t) = 0$ which leads to $h_1(t) \sim e^{-(1-p_\infty)t + \frac{p_0 - p_\infty}{1-\lambda}(1 - e^{-(1-\lambda)t})}$. This exponential decay happens to be faster than the second order contribution, which is also exponential $h_2(t) \sim e^{s_2^* t}$, and thus for long enough time the second order prevails.

Combining the results of this subsection with those of Section 5.2, we conclude that if the activation probabilities p_i tend to a non-null value $p_\infty > 0$, then the system always orders and tends to a consensus state in the aging case (a decreasing function p_i) but it does not order in the anti-aging situation of an increasing function p_i.

6. Summary and conclusions

In this work we have studied memory effects (aging and anti-aging) in an opinion dynamics model, by means of analytical and numerical approaches. More specifically, we have focused on a mean-field (all-to-all) description of the voter model, where the influence of the aging of the individuals has been modeled through the activation probability, p_i, or the copying probability of the individuals as a function of their internal age i. Overall, we have shown that the functional form of p_i has a crucial impact on how and whether the system reaches consensus or not. For the sake of concreteness, we have employed in our analysis monotonic functions p_i with three parameters: p_0 (or p_i for zero age), p_∞ (or p_i for ∞ age), and a third one, c or λ, tuning the transition $p_0 \to p_\infty$.

When the activation probability is constant $p_0 = p_\infty$, we recover the original non-aging voter model. In this case, the system keeps its initial magnetization, for an infinite time in the thermodynamic limit or for a characteristic time T that scales with the number of agents. If the activation probability is not constant and tends to a nonzero value for large ages, $p_0 \neq p_\infty > 0$, the aging and anti-aging cases produce opposite effects in the dynamics. On the one hand, for the case of aging, with $p_0 > p_\infty > 0$, the system orders with an exponential decay of the fraction $x(t)$ of individuals in the state $+1$ towards one of the consensus states $x(t) \to 0, 1$. On the other hand, for the anti-aging case, with $0 < p_0 < p_\infty$, the system reaches coexistence with $x \to 1/2$.

As explained in Ref. [47], the results for $p_\infty > 0$ can be understood heuristically: the aging mechanism amplifies any small asymmetry in the initial conditions. Take an initial condition close to consensus, say $x = 0$, and all the agents with

zero age. Then, the systems evolves in a first, very short stage as if no aging was present since all agents have the same herding rate. After the first transitions, most of the agents become older in the state -1, while a small fraction are younger with states ± 1. From a dynamical point of view, the only difference between the latter situation and the voter model is in the presence of the small fraction of the young agents. In the case of aging, since the rate of changing state is bigger for the young agents, the most probable event is that a young agent copies the state of an old one. Altogether, the fraction $x(t)$ of individuals in the state $+1$ decreases. On the contrary, for the case of anti-aging with the young agents having smaller rates, the most probable event is that of an old copying a young and, hence, the same fraction $x(t)$ increases.

For the case of aging with zero p_∞, $p_0 > p_\infty = 0$, the system may or may not order, depending on how fast is the decay of p_i to zero as the age increases. From the theoretical analysis of the integro-differential equations close to the consensus state, together with the results of numerical simulations, we infer the following criterion: if p_i decays faster than $1/i$ then the system gets trapped in a frozen state given by the initial conditions, while the system orders in other cases. The decay $p_i \sim 1/i$ can be then regarded as a critical functional form where we proved that the system orders with a power-law time dependence.

The results of $p_\infty = 0$ can also be understood using qualitative arguments. The evolution of the magnetization can be explained as for the case $p_\infty > 0$, the only difference now being the time needed for the system to reach its final value. For p_i decaying slow enough, the system reaches consensus but on a time much larger than that for $p_\infty > 0$, since it takes more time to convince all agents, specially the older ones. For the other case of p_i decaying faster, almost all agents become zealots [38] on a short time scale, and the system gets frozen on an active state, $x \neq 0, 1$, in general.

The results of this paper have considered, for mathematical convenience, the all-to-all connectivity. It would be interesting to extend these results to the case where the connectivity is defined by a complex network structure in the interactions between nodes, along the lines developed in [24], although the consideration of the two effects, topology and memory, is a very challenging problem from the theoretical point of view. A first step would be to characterize the power law exponent $x(t) \sim t^{-\beta}$, which shows a strong dependence on the network as numerically proved in [48]. Also, it has not been properly studied yet the aging version of the voter model in low dimensions. Questions such as the ordering mechanism in a lattice, if there is growth of domains or not has not been addressed in detail. Research in progress [67] concerns the extension of these results to the noisy version of the voter model where agents have a finite probability of switching states independently of the state of the neighbors.

Acknowledgments

Partial financial support has been received from the Agencia Estatal de Investigacion (AEI, Spain) and Fondo Europeo de Desarrollo Regional (FEDER,UE) under Project PACSS RTI2018-093732-B-C21 and the María de Maeztu Program for units of Excellence in R&D, Spain (MDM-2017-0711). A. F. P. acknowledges support by the Formación de Profesorado Universitario, Spain (FPU14/00554) program of Ministerio de Educación, Cultura y Deportes (MECD) (Spain). We thank J. F. Gracia for valuable discussions concerning the results of Ref. [48].

Appendix A. Asymptotic expansions

A.1.

If we use the expression Eq. (1) for the activation probabilities, we obtain explicit expressions for the functions defined in Eqs. (21), (22)

$$G(t) = (1-p_0)e^{-t}M\left(1 + c\frac{1-p_0}{1-p_\infty}, 1+c, (1-p_\infty)t\right), \tag{A.1}$$

$$L(t) = e^{-t}\left[p_0 M\left(c, c+1, t\right) + t\frac{p_\infty}{1+c}M\left(1+c, 2+c, t\right)\right], \tag{A.2}$$

where $M(\alpha, \beta, x)$ is Kummer's ${}_1F_1(\alpha; \beta; x)$ confluent hypergeometric function. Using the expansion for large z: $M(\alpha, \beta, z) \sim \frac{\Gamma(\beta)}{\Gamma(\alpha)} e^z z^{\alpha-\beta}$ we obtain in the asymptotic limit $t \to \infty$ the expansions:

$$G(t) \sim Ae^{-p_\infty t}t^{-b}, \tag{A.3}$$

$$L(t) \sim \frac{p_0 c}{t} + p_\infty, \tag{A.4}$$

$$A = (1-p_\infty)\frac{\Gamma(c)}{\Gamma\left(c\frac{1-p_0}{1-p_\infty}\right)}, \tag{A.5}$$

$$b = c\frac{p_0 - p_\infty}{1-p_\infty}. \tag{A.6}$$

Please cite this article as: A.F. Peralta, N. Khalil and R. Toral, Ordering dynamics in the voter model with aging, Physica A (2019) 122475, https://doi.org/10.1016/j.physa.2019.122475.

The expressions for $G(t)$ assume $p_\infty \neq 1$. For $p_\infty = 1$ we find

$$G(t) = \Gamma(c)(c(1-p_0))^{1-c/2} e^{-t} t^{-c/2} I_c\left(2\sqrt{c(1-p_0)t}\right) \tag{A.7}$$

$$\sim \frac{\Gamma(c)}{\sqrt{2\pi\sqrt{2}}}[c(1-p_0)]^{(3-2c)/4} t^{-(c+2)/4} e^{-t}. \tag{A.8}$$

It is also possible to obtain the Laplace transform of $G(t)$ as:

$$\hat{G}(s) = \frac{1-p_0}{1+s}\, {}_2F_1\left[1, 1+c\frac{1-p_0}{1-p_\infty}; 1+c; \frac{1-p_\infty}{1+s}\right]. \tag{A.9}$$

A.2.

In the case of activation probabilities given by Eq. (2) it is possible to obtain $L(t)$ analytically:

$$L(t) = (p_0 - p_\infty)e^{-(1-\lambda)t} + p_\infty, \tag{A.10}$$

although we have not been able to find a closed expression for $G(t)$,

$$G(t) = e^{-t} \sum_{i=0}^{\infty} \frac{(1-p_\infty)^{i+1}\left(\frac{p_0-p_\infty}{1-p_\infty}; \lambda\right)_{i+1}}{i!} t^i, \tag{A.11}$$

with $(q; a)_n$ the q-Pochhammer symbol [71]. It is possible, however, to obtain the asymptotic expansion for $t \to \infty$ as

$$G(t) \sim (1-p_\infty)\left(\frac{p_0-p_\infty}{1-p_\infty}; \lambda\right)_\infty e^{-p_\infty t}. \tag{A.12}$$

In the particular case $p_\infty = 0$ it yields $G(t) \sim (p_0; \lambda)_\infty$.

Finally, we mention the Laplace transform of $G(t)$ as:

$$\hat{G}(s) = \sum_{i=0}^{\infty} \left(\frac{1-p_\infty}{1+s}\right)^{i+1} \left(\frac{p_0-p_\infty}{1-p_\infty}; \lambda\right)_{i+1}. \tag{A.13}$$

For the numerical calculation of $G(t)$ and $\hat{G}(s)$ in this case we use Eqs. (A.11), (A.13) using a sufficiently large number of terms in the sums.

Appendix B. Solution of Eqs. (19), (20) using Eqs. (31), (32)

If $G(t) \equiv G_\infty$ is a constant, we can differentiate Eq. (19) and obtain a system of differential equations:

$$\frac{dx}{dt} = \frac{dx_0^+}{dt} + G_\infty x_0^+(t), \tag{B.1}$$

$$\frac{dx_0^+}{dt} = -x_0^+ + L(t)x(t). \tag{B.2}$$

From the last equation we get $x(t) = \left(\frac{dx_0^+}{dt} + x_0^+\right)/L(t)$ which, replaced in Eq. (B.1) leads to a closed second order linear differential equation for $x_0^+(t)$. The change of variables $z \equiv -\frac{p_0}{1-\lambda} e^{-(1-\lambda)t}$ makes the coefficients of the equation to be simple polynomials and a standard technique based on Frobenius power-series expansion leads to the general solution $x(t) = \left[c_1 x^{(1)}(t) + c_2 x^{(2)}(t)\right] x(0)$, $x_0^+(t) = \left[c_1 x_0^{(1)}(t) + c_2 x_0^{(2)}(t)\right] x(0)$, where c_1 and c_2 are constants imposed by satisfying the initial condition $x(0) = x_0^+(0) = 1$, and

$$x_0^{(1)}(t) = e^{-t} M\left(\frac{1-G_\infty}{1-\lambda}, \frac{1}{1-\lambda}, -\frac{p_0}{1-\lambda} e^{-(1-\lambda)t}\right), \tag{B.3}$$

$$x_0^{(2)}(t) = e^{-(1-\lambda)t} M\left(1 - \frac{G_\infty}{1-\lambda}, \frac{1-2\lambda}{1-\lambda}, -\frac{p_0}{1-\lambda} e^{-(1-\lambda)t}\right), \tag{B.4}$$

$$x^{(1)}(t) = (1-G_\infty)e^{-t} M\left(1 + \frac{1-G_\infty}{1-\lambda}, \frac{2-\lambda}{1-\lambda}, -\frac{p_0}{1-\lambda} e^{-(1-\lambda)t}\right), \tag{B.5}$$

$$x^{(2)}(t) = \frac{\lambda}{p_0} M\left(1 - \frac{G_\infty}{1-\lambda}, \frac{1-2\lambda}{1-\lambda}, -\frac{p_0}{1-\lambda} e^{-(1-\lambda)t}\right) + \tag{B.6}$$

$$\frac{1-\lambda-G_\infty}{1-2\lambda} e^{-(1-\lambda)t} M\left(2 - \frac{G_\infty}{1-\lambda}, \frac{2-3\lambda}{1-\lambda}, -\frac{p_0}{1-\lambda} e^{-(1-\lambda)t}\right). \tag{B.7}$$

Please cite this article as: A.F. Peralta, N. Khalil and R. Toral, Ordering dynamics in the voter model with aging, Physica A (2019) 122475, https://doi.org/10.1016/j.physa.2019.122475.

In the limit $t \to \infty$, the asymptotic behavior is

$$x_0^{(1)}(t) \to e^{-t}, \tag{B.8}$$

$$x_0^{(2)}(t) \to e^{-(1-\lambda)t}, \tag{B.9}$$

$$x^{(1)}(t) \to (1 - G_\infty)e^{-t}, \tag{B.10}$$

$$x^{(2)}(t) \to \frac{\lambda}{p_0}, \tag{B.11}$$

leading to

$$x_0^{+}(t) \to x(0)c_2 e^{-(1-\lambda)t}, \tag{B.12}$$

$$x(t) \to x(0)c_2 \frac{\lambda}{p_0}. \tag{B.13}$$

We do not reproduce the explicit expressions for the constants c_1 and c_2 as they are too long and not very illuminating. It suffices to say that in the case $\lambda = 1/2$, $p_0 = 1/2$ used in Section 5.3 it is $c_2 = 1/2$.

References

[1] R. Pastor-Satorras, A. Vespignani, Epidemic spreading in scale-free networks, Phys. Rev. Lett. 86 (14) (2001) 3200.
[2] R. Pastor-Satorras, C. Castellano, P. Van Mieghem, A. Vespignani, Epidemic processes in complex networks, Rev. Modern Phys. 87 (3) (2015) 925.
[3] D.M. Abrams, S.H. Strogatz, Linguistics: Modelling the dynamics of language death, Nature 424 (6951) (2003) 900.
[4] X. Castelló, V.M. Eguíluz, M. San Miguel, Ordering dynamics with two non-excluding options: bilingualism in language competition, New J. Phys. 8 (12) (2006) 308.
[5] D. Stauffer, X. Castelló, V.M. Eguiluz, M. San Miguel, Microscopic Abrams–Strogatz model of language competition, Physica A 374 (2) (2007) 835–842.
[6] F. Vazquez, X. Castelló, M. San Miguel, Agent based models of language competition: Macroscopic descriptions and order–disorder transition, J. Stat. Mech. Theory Exp. (2010).
[7] A. Kirman, Ants, rationality, and recruitment, Quart. J. Econ. 108 (1993) 137.
[8] S. Alfarano, T. Lux, F. Wagner, Time estimation of agent-based models: The case of an asymmetric Herding model, Comput. Econ. 26 (2005) 19.
[9] S. Alfarano, T. Lux, F. Wagner, Time variation of higher moments in a financial market with heterogeneous agents: An analytical approach, Econ. Dyn. Control 32 (2008) 101.
[10] S. Alfarano, M. Milaković, Network structure and N-dependence in agent-based herding models, J. Econom. Dynam. Control 33 (2009) 78.
[11] V. Gontis, A. Kononovicius, Spurious memory in non-equilibrium stochastic models of imitative behavior, Entropy 19 (2017) 387.
[12] A. Carro, R. Toral, M. San Miguel, Markets, herding and response to external information, PLoS One 10 (7) (2015) e0133287.
[13] A. Kononovicius, J. Ruseckas, Order book model with herd behavior exhibiting long-range memory, Physica A 525 (2019) 171–191.
[14] A.L. Vilela, C. Wang, K.P. Nelson, H.E. Stanley, Majority-vote model for financial markets, Physica A 515 (2019) 762–770.
[15] A. Barrat, M. Barthelemy, A. Vespignani, Dynamical Processes on Complex Networks, Cambridge university press, 2008.
[16] C. Castellano, S. Fortunato, V. Loreto, Statistical physics of social dynamics, Rev. Modern Phys. 81 (2) (2009) 591.
[17] J. Fernández-Gracia, K. Suchecki, J.J. Ramasco, M. San Miguel, V.M. Eguíluz, Is the voter model a model for voters? Phys. Rev. Lett. 112 (2014) 158701.
[18] P. Clifford, A. Sudbury, A model for spatial conflict, Biometrika 60 (3) (1973) 581–588.
[19] R.A. Holley, T.M. Liggett, Ergodic theorems for weakly interacting infinite systems and the voter model, Ann. Probab. 3 (4) (1975) 643–663.
[20] F. Vazquez, V.M. Eguíluz, Analytical solution of the voter model on uncorrelated networks, New J. Phys. 10 (6) (2008) 063011.
[21] S. Redner, Reality inspired voter models: A mini-review, C. R. Phys. (2019) http://dx.doi.org/10.1016/j.crhy.2019.05.004.
[22] P.L. Krapivsky, S. Redner, E. Ben-Naim, A Kinetic View of Statistical Physics, Cambridge University Press, 2010.
[23] T.M. Liggett, Interacting Particle Systems, Vol. 276, Springer Science & Business Media, 2012.
[24] A.F. Peralta, A. Carro, M. San Miguel, R. Toral, Stochastic pair approximation treatment of the noisy voter model, New J. Phys. 20 (2018) 103045.
[25] A. Carro, R. Toral, M. San Miguel, The noisy voter model on complex networks, Sci. Rep. 6 (2016) 24775.
[26] P. Nyczka, K. Sznajd-Weron, J. Cisło, Phase transitions in the q-voter model with two types of stochastic driving, Phys. Rev. E 86 (2012) 011105.
[27] P. Nyczka, K. Sznajd-Weron, Anticonformity or independence?—Insights from statistical physics, J. Stat. Phys. 151 (1) (2013) 174–202.
[28] A. Jędrzejewski, Pair approximation for the q-voter model with independence on complex networks, Phys. Rev. E 95 (2017) 012307.
[29] A.F. Peralta, A. Carro, M. San Miguel, R. Toral, Analytical and numerical study of the non-linear noisy voter on complex networks, Chaos 28 (2018) 075516.
[30] A.R. Vieira, C. Anteneodo, Threshold q-voter model, Phys. Rev. E 97 (2018) 052106.
[31] F. Vazquez, V.M. Eguíluz, M. San Miguel, Generic absorbing transition in coevolution dynamics, Phys. Rev. Lett. 100 (2008) 108702.
[32] M. Diakonova, M. San Miguel, V.M. Eguíluz, Absorbing and shattered fragmentation transitions in multilayer coevolution, Phys. Rev. E 89 (2014) 062818.
[33] M. Diakonova, V.M. Eguíluz, M. San Miguel, Noise in coevolving networks, Phys. Rev. E 92 (2015) 032803.
[34] T. Raducha, B. Min, M. San Miguel, Coevolving nonlinear voter model with triadic closure, Europhys. Lett. 124 (3) (2018) 30001.
[35] B. Min, M. San Miguel, Multilayer coevolution dynamics of the nonlinear voter model, New J. Phys. 21 (3) (2019) 035004.
[36] F. Herrerías-Azcué, T. Galla, Consensus and diversity in multi-state noisy voter models, Phys. Rev. E 100 (2019) 022304.
[37] F. Vazquez, E.S. Loscar, G. Baglietto, A multi-state voter model with imperfect copying, 2019, arXiv arXiv:1902.07253.
[38] N. Khalil, M. San Miguel, R. Toral, Zealots in the mean-field noisy voter model, Phys. Rev. E 97 (2018) 012310.
[39] N. Khalil, R. Toral, The noisy voter model under the influence of contrarians, Physica A 515 (2019) 81–92.
[40] A. Jędrzejewski, K. Sznajd-Weron, Impact of memory on opinion dynamics, Physica A 505 (2018) 306–315.
[41] B. Min, K.i. Goh, I.m. Kim, Suppression of epidemic outbreaks with heavy-tailed contact dynamics, Europhys. Lett. 103 (2013) 50002.
[42] M. Boguñá, L. Lafuerza, R. Toral, M.Á. Serrano, Simulating non-Markovian stochastic processes, Phys. Rev. E 90 (2014) 042108.
[43] M. Starnini, J.P. Gleeson, M. Boguñá, Equivalence between non-Markovian and Markovian dynamics in epidemic spreading processes, Phys. Rev. Lett. 118 (2017) 128301.

Please cite this article as: A.F. Peralta, N. Khalil and R. Toral, Ordering dynamics in the voter model with aging, Physica A (2019) 122475, https://doi.org/10.1016/j.physa.2019.122475.

[44] S.P. Blythe, R.M. Anderson, Variable infectiousness in HIV transmission models, Math. Med. Biol. 5 (1988) 181.
[45] N.G. van Kampen, Remarks on non-Markov processes, Braz. J. Phys. 28 (1998) 90.
[46] J. Łucza, Non-markovian stochastic processes: Colored noise, Chaos 15 (2005) 026107.
[47] H.-U. Stark, C.J. Tessone, F. Schweitzer, Decelerating microdynamics can accelerate macrodynamics in the voter model, Phys. Rev. Lett. 101 (2008) 018701.
[48] J. Fernández-Gracia, V.M. Eguíluz, M. San Miguel, Update rules and interevent time distributions: Slow ordering versus no ordering in the voter model, Phys. Rev. E 84 (1) (2011) 015103.
[49] E. Ben-Naim, L. Frachebourg, P.L. Krapivsky, Coarsening and persistence in the voter model, Phys. Rev. E 53 (4) (1996) 3078.
[50] V. Sood, S. Redner, Voter model on heterogeneous graphs, Phys. Rev. Lett. 94 (17) (2005) 178701.
[51] K. Suchecki, V.M. Eguíluz, M. San Miguel, Voter model dynamics in complex networks: Role of dimensionality, disorder, and degree distribution, Phys. Rev. E 72 (3) (2005) 036132.
[52] T. Pérez, K. Klemm, V.M. Eguíluz, Competition in the presence of aging: dominance, coexistence, and alternation between states, Sci. Rep. 6 (2016) 21128.
[53] A.C.R. Martins, S. Galam, Building up of individual inflexibility in opinion dynamics, Phys. Rev. E 87 (2013) 042807.
[54] O. Artime, A.F. Peralta, R. Toral, J.J. Ramasco, M. San Miguel, Aging-induced phase transition, Phys. Rev. E 98 (2018) 032104.
[55] O. Artime, A. Carro, A.F. Peralta, J.J. Ramasco, M. San Miguel, R. Toral, Herding and idiosyncratic choices: Nonlinearity and aging-induced transitions in the noisy voter model, C. R. Phys. (2019) http://dx.doi.org/10.1016/j.crhy.2019.05.003, in press.
[56] D. Considine, S. Redner, H. Takayasu, Comment on noise-induced bistability in a Monte Carlo surface-reaction model, Phys. Rev. Lett. 63 (1989) 2857.
[57] B.L. Granovsky, N. Madras, The noisy voter model, Stochastic Process. Appl. 55 (1995) 23.
[58] Y. Wu, C. Zhou, J. Xiao, J. Kurths, H.J. Schellnhuber, Evidence for a bimodal distribution in human communication, Proc. Natl. Acad. Sci. USA 107 (2010) 18803.
[59] J. Candia, M.C. González, P. Wang, T. Schoenharl, G. Madey, A. Barabási, Uncovering individual and collective human dynamics from mobile phone records, J. Phys. A 41 (2008) 224015.
[60] O. Artime, J.J. Ramasco, M. San Miguel, Dynamics on networks: competition of temporal and topological correlations, Sci. Rep. 7 (2017) 41627.
[61] O. Artime, J.F. Gracia, J.J. Ramasco, M. San Miguel, Joint effect of ageing and multilayer structure prevents ordering in the voter model, Sci. Rep. 7 (2017) 7166.
[62] D. Escaff, R. Toral, C. Van Den Broeck, K. Lindenberg, A continuous-time persistent random walk model for flocking, Chaos 28 (7) (2018) 075507.
[63] O. Artime, N. Khalil, R. Toral, M. San Miguel, First-passage distributions for the one-dimensional Fokker–Planck equation, Phys. Rev. 98 (2018) 042143.
[64] N. van Kampen, Stochastic Processes in Physics and Chemistry, third ed., North-Holland, Amsterdam, 2007.
[65] R. Toral, P. Colet, Stochastic Numerical Methods: An Introduction for Students and Scientists, Wiley, 2014, URL http://eu.wiley.com/WileyCDA/WileyTitle/productCd-3527411496html.
[66] A.F. Peralta, R. Toral, System-size expansion of the moments of a master equation, Chaos 28 (2018) 106303.
[67] A.F. Peralta, N. Khalil, R. Toral, Reduction to Markovian dynamics: The case of aging in the noisy voter model, 2019, in preparation.
[68] J. Ozaita, Noisy Voter Model with Partial Aging and Anti-Aging (Master's thesis), University of the Balearic Islands, Palma, Spain, 2018, https://ifisc.uib-csic.es/en/publications/noisy-voter-model-with-partial-aging-and-anti-agin/.
[69] A. Arikoglu, I. Ozkol, Solutions of integral and integro-differential equation systems by using differential transform method, Comput. Math. Appl. 56 (9) (2008) 2411–2417.
[70] J.T. Day, Note on the numerical solution of integro-differential equations, Comput. J. 9 (4) (1967) 394–395.
[71] URL https://en.wikipedia.org/wiki/Q-Pochhammer_symbol.

Please cite this article as: A.F. Peralta, N. Khalil and R. Toral, Ordering dynamics in the voter model with aging, Physica A (2019) 122475, https://doi.org/10.1016/j.physa.2019.122475.